ACS OMEGA

http://pubs.acs.org/journal/acsodf

Article

Dehydroroyleanone as a Building Block for a Drug Delivery Platform Based on Self-Assembled Nanoparticles: Structural Studies and Chemical Modification

Catarina García, Carlos E. S. Bernardes, M. Fátima M. Piedade, Gaia Fumagalli, Eleonora Colombo, Ana M. Díaz-Lanza, Catarina P. Reis, Isabel Correia, Lia Ascensão, Daniele Passarella, Manuel E. Minas da Piedade,* and Patrícia Rijo*

Cite This: *ACS Omega* 2022, 7, 44180−44186

Read Online

ACCESS | Metrics & More | Article Recommendations | Supporting Information

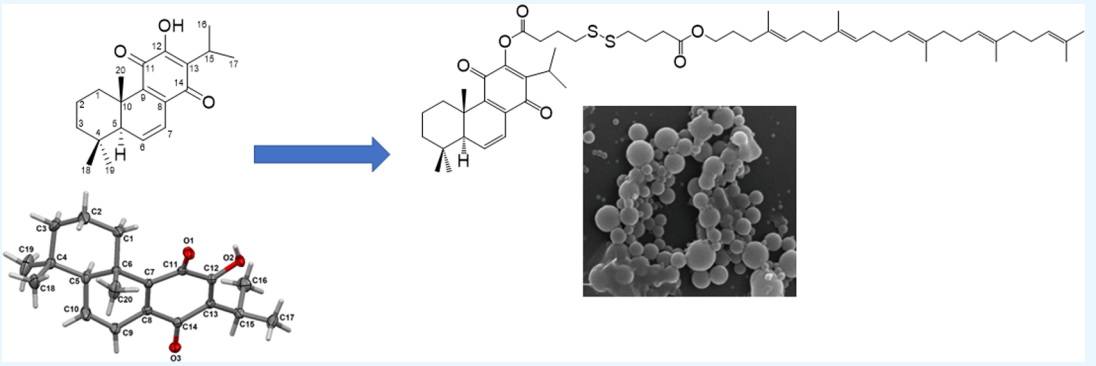

ABSTRACT: 6,7-Dehydroroyleanone (DHR) is a caspase-induced cytotoxic abietane diterpene, frequently found on *Plectranthus* spp. A pharmaceutical formulation consisting of a DHR-squalene conjugate was synthesized and analyzed by different techniques such as scanning electron microscopy (SEM). The facile production of the dispersion of DHR-squalene conjugate nanoparticles in phosphate buffer (pH 7.4) suggests that this nanodelivery platform may be an effective system to improve the solubility and bioavailability of DHR, so that therapeutical systemic levels may be achieved.

INTRODUCTION

6,7-Dehydroroyleanone (DHR, Figure 1) is an abietane diterpene that can be isolated from the essential oil of

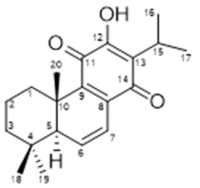

Figure 1. Molecular structure of 6,7-dehydroroyleanone (DHR).

Plectranthus madagascariensis (Pers.) Benth. Its bioactivity has been recently studied and found to be intimately related to cytotoxic properties and effects on cell death-related targets.[1] DHR activates the intrinsic apoptotic pathway and can evade *P*-glycoprotein-related mechanisms of resistance, which is itself biologically significant.[1] Several commercially available chemotherapeutic agents (such as paclitaxel) fail to do so, thus inducing resistance and compromising therapeutic action.[1] Nevertheless, when it comes to finding effective treatments for cancer, the observation of high cytotoxic parameters is often insufficient to ensure that a new medicine can be successfully produced. Three other important aspects that need to be considered at the outset of drug development based on solid active pharmaceutical ingredients (APIs) are the structural, thermal, and solubility properties of the lead compound. Indeed, both the crystal structure and thermal behavior are intimately related to phenomena such as polymorphism and chemical decomposition, which have a strong influence on solubility, dissolution rate, stability, shelf life, and other key properties that must be strictly controlled to warrant the manufacture of a reproducible and safe pharmaceutical product.[2−5] The possibility of low aqueous solubility, low partition coefficient, and heavy exportation via efflux trans-

Received: September 1, 2022
Accepted: November 9, 2022
Published: November 23, 2022

https://doi.org/10.1021/acsomega.2c05353
ACS Omega 2022, 7, 44180−44186

porters (e.g., *P*-glycoprotein) deserves also assessment, since all of these features can negatively influence the drug intracellular uptake and overall performance. Finding strategies for solubility improvement has become a major objective within this scope since it has been estimated that ca. 90% of the compounds in current pharmaceutical development pipelines display low aqueous solubility.[6] Such strategies can allow the compound to reach the therapeutic concentration using a lower dose and reduce adverse side effects associated with excess drug that remains in the system without reaching the desired target. Thermal characterization is also important in this regard since solubility enhancement procedures that rely on the production of an amorphous material by, e.g., melting and quench cooling or dispersion in polymeric excipients cannot be used if fusion is accompanied by chemical decomposition.

Nanodelivery platforms have been emerging as a way to successfully overcome the latter issues and obtain better therapeutic effectiveness while minimizing toxic side effects.[7−9] Within this scope, lipid−drug conjugates (LDCs), also dubbed lipoidal prodrugs, have gained increasing attention as effective drug carriers and solubility/bioavailability enhancers.[9−12] These self-assembled nanoparticle systems, which normally contain the drug covalently attached to a lipid moiety, can also profit from the pathways of lipid biochemistry to target specific organs depending on the nanoparticle size.[9]

In this work, the structure, thermal stability, tendency for polymorphism, and solubility (phosphate buffer, pH 7.4, 298 and 310 K) of DHR have been investigated. A lipid-DHR conjugate was also synthesized and used to prepare a water-dispersible nanoparticle formulation as a means to enhance the aqueous solubility of DHR.

EXPERIMENTAL SECTION

6,7-Dehydroroyleanone was isolated from the essential oil of *P. madagascariensis* as previously described[1] by flash chromatography in silica gel (Merck, 240−400 Mesh). Recrystallization from methanol (Merck, 98.5%) afforded orange-reddish crystals. Optical rotation measurements in $CHCl_3$ (Merck, ≥99.8%) led to $[\alpha]_D^{21} = -2.85°$. High-performance liquid chromatography (HPLC) analysis gave a purity of 96.9%.

HPLC analysis for purity assessment and determination of DHR solubility was performed as described in Garcia et al. 2018.[1] The HPLC grade water, chloroform (≥99.8%), dichloromethane (≥99.8%), acetone (≥99.9%), methanol (98.5%), and trifluoroacetic acid (≥99.0%) used in this work were obtained from Merck. Both the limit of detection (LOD) and limit of quantification (LOQs) were determined.

^{1}H- and ^{13}C-RMN spectra were recorded at 300 and 75 MHz, respectively, on Bruker DRX-300 spectrometers using $CDCl_3$ (Aldrich, 99.80%, <0.01% H_2O) as a solvent. Chemical shifts were determined using chloroform as a reference.

Human colon (HCT116) and breast (MCF-7) adenocarcinoma cell lines were purchased from ATCC. Both were cultured in RPMI-1640 medium with ultraglutamine (Lonza, VWR, Carnaxide, Portugal) and supplemented with 10% fetal bovine serum (FBS; Gibco, Alfagene, Carcavelos, Portugal). Cells were maintained at 310 K in a humidified atmosphere of 5% CO_2.

Chemical reactions were monitored by thin-layer chromatography (TLC) on precoated silica gel plates (Merck 60F_{254}). Detection was performed by exposing the developed plates to I_2 vapor or ultraviolet (UV) light (254 nm).

Electrospray ionization (ESI) mass spectrometry analysis was performed on a Thermo Fisher Finnigan LCQ Advantage apparatus.

Optical rotation measurements were carried out on an Optical Activity Lda AA-10R automatic polarimeter. The solvent was $CHCl_3$, and the cell had an optical path of 20 cm.

Circular dichroism (CD) spectra were measured on a Jasco J-720 spectropolarimeter (Jasco, Hiroshima, Japan) with a 175−800 nm photomultiplier (EXEL-308). The solvent was CH_2Cl_2, and the solutions were contained in a 1.0 cm quartz cuvette. Pure CH_2Cl_2 was used to perform the baseline subtraction. Each spectrum was recorded at room temperature in the range 220−600 nm with a scan rate of 200 nm min^{-1} and a resolution of 1 nm. The bandwidth was set at 1 nm, two scans were accumulated and averaged, and the response time was 2 s.

The molecular and crystal structures of 6,7-dehydroroyleanone were obtained from single-crystal X-ray diffraction experiments conducted at 167 ± 2 K on a Bruker AXS-KAPPA APEX II area detector diffractometer. Graphite-monochromated Mo Kα (λ = 0.71073 Å) radiation was used with the X-ray generator operated at 50 kV and 30 mA. The data collection was monitored with the APEX2 program.[13] The SAINT[13] and SADABS[13] programs were applied to correct all data for Lorentzian, polarization, and absorption effects. The structures were solved by direct methods with SHELXS[14] and refined by full-matrix least-squares on F^2 with SHELXL,[15] both included in WINGX-Version 1.80.05.[16] Non-hydrogen atoms were refined with anisotropic thermal parameters. All hydrogen atoms were located in a Fourier map, and their positions and isotropic displacement parameters, U_{iso}(H), were refined freely. Graphical representations were prepared using Mercury 3.10.1 (Build 168220).[17] PLATON[18] was used for hydrogen bond interactions. A summary of the crystal data, structure solution, and refinement parameters is given in Table S1 (Supporting Information).

Thermogravimetry (TG) and differential scanning calorimetry (DSC) analyses on DHR were carried out on PerkinElmer TGA7 and DSC 7 apparatuses, respectively.

The solubility of 6,7-dehydroroyleanone was tested as recommended in the European Pharmacopoeia 7.0. Two suspensions of DHA (∼1 mg) in phosphate buffer solution (pH 7.4) were prepared and kept under stirring (150 rpm) for 24 h, one at 298 K and the other at 310 K. For each assay, the supernatant liquid was subsequently analyzed by HPLC−DAD, according to a previously reported method.[1] Three independent measurements of each sample, under different conditions, were conducted (n = 3, mean ± standard deviation (SD)).

The synthesis of the DHR-squalene conjugate is summarized in Figure 2. Self-assembled nanoparticles were prepared by the solvent displacement method. The DHR-squalene conjugate (4 mg) was dissolved in acetone (1 cm^3) to give a yellow solution 4.42 mM in DHR. Nanoprecipitation was then induced by adding the solution dropwise and under stirring (400 rpm) to 2 cm^3 of Milli-Q water without surfactant addition. The organic solvent was removed under reduced pressure at 313 K. The turbid yellow suspension containing the nanoassemblies was stored in the dark at 277 K.

The particle diameter (d) and polydispersity index (PI) of the nanoassemblies were obtained by dynamic light scattering (DLS) using a Coulter Nano-Sizer Delsa TMNano C apparatus at a fixed angle of 90°. Sample **2** was subjected to

https://doi.org/10.1021/acsomega.2c05353
ACS Omega 2022, 7, 44180−44186

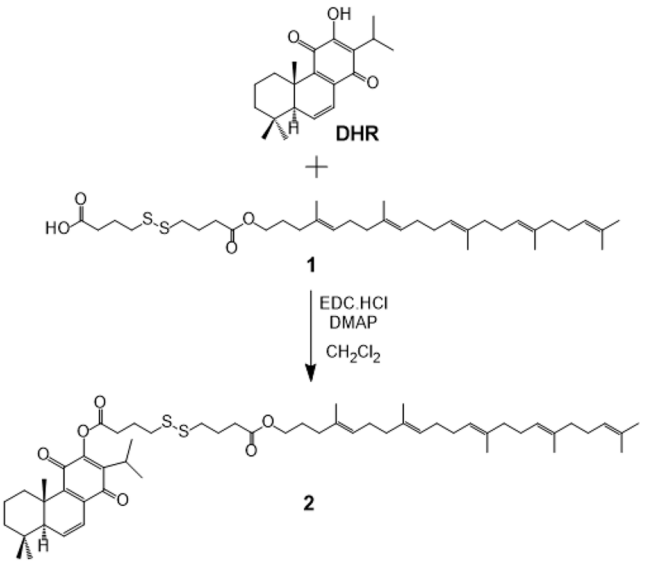

Figure 2. Coupling of 6,7-dehydroroyleanone (DHR) with a squalene-type chain using a labile linker.

a 1:40 (v/v) dilution with Milli-Q water before analysis, which was performed in triplicate, at 298 K. The ζ-potential was measured using a Malvern Zetasizer Nano S (Malvern Instruments, Worcestershire, U.K.). The stability of the preparation was assessed every week, for 2 months, based on the determination of the stability ratio (SR) given by

$$\mathrm{SR} = \frac{\zeta_t}{\zeta_{t=0}} \quad (1)$$

where $\zeta_{t=0}$ and ζ_t are the ζ-potentials determined at the beginning of the assessment process and at a given time t, respectively.

The morphology of the nanoassemblies was analyzed by scanning electron microscopy (SEM). Aliquots (10 μL) of the aqueous suspensions containing nanoparticles (NPs) were carefully dispersed over round glass coverslips previously coated with poly-L-lysine and attached to the microscope stubs. The samples were subsequently coated with a thin layer of gold and observed on a JEOL 5200LV scanning electron microscope (JEOL Ltd., Tokyo, Japan) at an accelerating voltage of 20 kV. Images were recorded digitally.

RESULTS AND DISCUSSION

The circular dichroism spectrum obtained for DHR in CH_2Cl_2 (Figure 3) shows bands at 251 nm (+12.07 M^{-1} cm^{-1}), ~270 nm (sh, +7.88 M^{-1} cm^{-1}), 329 nm (+1.26 M^{-1} cm^{-1}), and 472 nm (−1.81 M^{-1} cm^{-1}), which are in agreement with the measured UV−visible (UV−vis) absorption spectrum (data not shown). The CD spectrum exhibits many similarities with those reported for 7α-acetoxy-6β-hydroxyroyleanone (AHR)[19] and other related compounds.[20,21] The strong UV absorption at 251 nm is assigned to transitions in the *p*-benzoquinone chromophore. Enantiomers have CD spectra which are roughly mirror images. The intense spectrum shown in Figure 3, therefore, suggests that the DHR sample studied here predominantly corresponds to a specific enantiometer. The lack of pure enantiomeric standards precluded, however, the quantification of the enantiomeric purity.

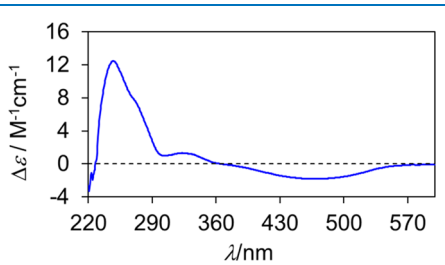

Figure 3. Circular dichroism spectrum measured for DHR in CH_2Cl_2 and 1 cm optical path.

The molecular structure of DHR and the corresponding atom labeling scheme are illustrated in Figure 4. Comparison

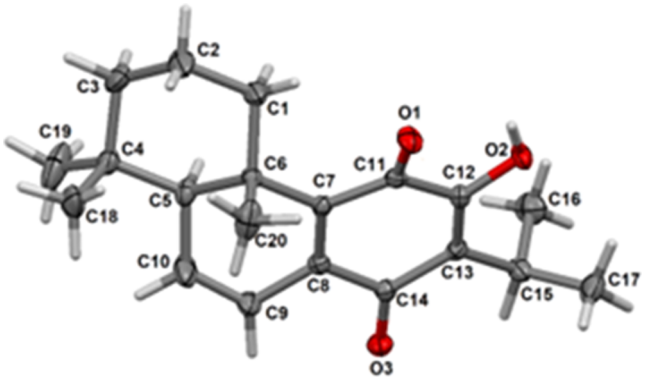

Figure 4. Molecular structure of 6,7-dehydroroyleanone (DHR) with the atom labeling scheme. Ellipsoids are set at 50% probability.

of the geometrical parameters with those previously reported for royleanone at 100 K[22] and for 7α-acetoxy-6β-hydroxyroyleanone (AHR) at 167 and 296 K[19] indicates that analogous bond distances and angles are similar in the three compounds, except for C9−C10, which in DHA has a double bond character (1.338 Å in DHR vs 1.514 Å for royleanone and 1.516 Å for AHR).

The DHR molecule has three fused six-membered rings typical of diterpenoid compounds. Two of them are *trans*-fused cyclohexane rings. The (C1−C6) ring is in a standard chair conformation with puckering parameters[23] Q = 0.5581 Å, θ = 4.12°, and φ = 15.82°, whereas the (C5−C10) one adopts a half chair conformation with puckering parameters Q = 0.4778 Å, θ = 114.91°, and φ = −157.97°. The Q, θ, and φ values for the C1−C6 ring are somewhat similar to those found in royleanone[22] and AHR.[19] This is not true, however, for the C5−C10 ring, probably because of the double bond character of C9−C10 in DHR.

The crystalline packing of DHR is formed by infinite planar $C_1^1(6)$ chains along the *b* axis (Figure 5), which are sustained by O−H···O hydrogen bonds ($d_{O_2H\cdots O_3}$ = 2.320 Å). This type of chain is also found in royleanone[22] and other royleanone derivatives such as 7α-acetoxy-6β-hydroxyroyleanone.[19] The crystalline packing of DHR is completed by the interaction of adjacent chains through weak C−H···O hydrogen bond interactions ($d_{C_{20}H\cdots O_3}$ = 2.59 Å and $d_{C_{20}H\cdots O_2}$ = 2.70 Å).

DSC experiments evidenced only a single peak when a DHR sample was heated from 303 to 450 K at a rate of 5 K min^{-1} (1st run in Figure 6). This peak, which corresponds to fusion, was characterized by onset (T_{on}) and maximum (T_{max}) temperatures T_{on} = 439.6 ± 0.2 K and T_{max} = 442.1 ± 0.2 K, respectively. The associated molar enthalpy and entropy of

https://doi.org/10.1021/acsomega.2c05353
ACS Omega 2022, 7, 44180−44186

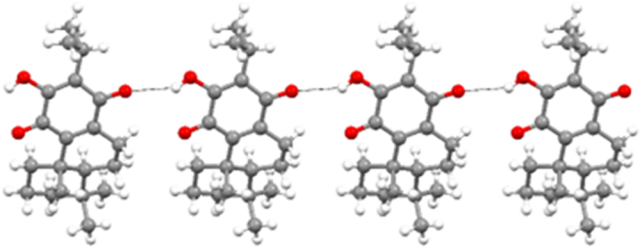

Figure 5. Infinite $C_1^1(6)$ chain motif in the crystal packing of 6,7-dehydroroyleanone (DHR).

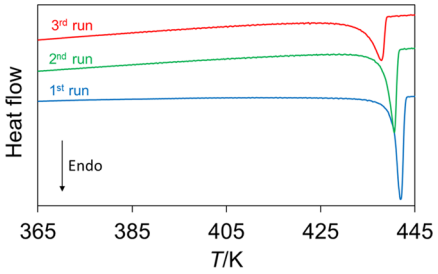

Figure 6. Differential scanning calorimetry curves obtained for 6,7-dehydroroyleanone (DHR) in three consecutive runs carried out in the range of 303−450 K at a heating rate of 5 K min^{-1}.

fusion were $\Delta_{fus}H_m$ = 29.9 ± 0.8 kJ mol^{-1} and $\Delta_{fus}S_m$ = 67.9 ± 0.8 J K^{-1} mol^{-1}, respectively. Note that the assigned uncertainties correspond to twice the standard error of the mean of four independent determinations. Fusion occurs with partial decomposition. This is evidenced by changes in the measured curves typically associated with such processes, namely, (i) the considerable broadening of the fusion peak and (ii) the progressive decrease of the onset temperature (∼2.5 K) and enthalpy of fusion (∼30%) observed after a sample crystallized from melt was reheated twice to 513 K (runs 2 and 3 in Figure 6).

The TG experiments in the range of 290−620 K (Figure 7) showed also a significant mass loss above the fusion onset

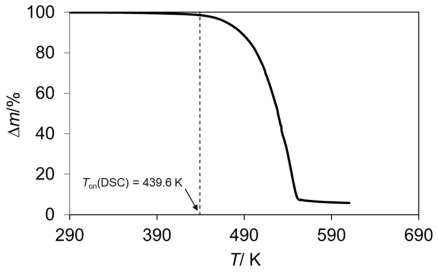

Figure 7. Typical TG curve obtained for 6,7-dehydroroyleanone (DHR) in the range of 303−450 K at a heating rate of 5 K min^{-1}. Note the significant mass loss observed after the fusion onset detected by DSC.

detected by DSC (439.6 K). This mass loss was found to correspond to both thermal decomposition (also detected by DSC) and vaporization.

Overall, two key conclusions can be drawn from the thermal analysis studies: (i) The fact that no solid−solid phase transitions were observed by DSC when DHR was heated from close to ambient temperature to the melting point suggests that polymorphism is not likely to be an issue if the compound is subjected to heat treatment within this range during the development of a pharmaceutical formulation. (ii) The observed partial decomposition of DHR noted on fusion precludes, however, the use of strategies to improve its solubility that involve melting, such as the production of glassy materials by quench cooling, or the preparation of some dispersions in polymeric excipients. This latter finding and the insolubility of DHR in aqueous media discussed in the next paragraph motivated the preparation of the nanodelivery platform described in this work.

The solubility of DHR in phosphate buffer (pH 7.4) was evaluated by keeping two 1 mg suspensions of the compound under stirring in this media, for 24 h, at 298 and 310 K, respectively. The HPLC−DAD analysis of the supernatant solution carried out at the end of the experiments showed no evidence of DHR dissolution at both temperatures. Given that the estimated limit of detection (LOD) and limit of quantitation (LOQ) of the technique were LOD = 4.43 × 10^{-6} μg cm^{-3} and LOQ = 1.34 × 10^{-5} μg cm^{-3}, respectively, (see the Experimental Section); this is in line with: (i) the high value of log*P* estimated using ChemDraw (v15.1; CambridgeSoft), which suggests that DHR is hydrophobic, hence poorly soluble in water; (ii) the calculated value of the partition coefficient (*clogP* = 5.06), which also indicates a low aqueous solubility. To overcome this problem nanoassemblies containing DHR were prepared as described in the next paragraph.

It is well known that besides the bioavailability improvement of insoluble drugs, nanoparticles are able to provide a focused drug delivery to a targeted site due to an enhanced permeation and retention (EPR) effect that allows tissue absorption of small molecules.[24] This focused drug delivery reduces the incidence of potential side toxic effects.[24]

The encapsulation of abietane diterpenes in nanoparticles for drug delivery purposes has been reported.[25] Nonetheless, to the best of our knowledge, the induction of self-assemblies containing these compounds has not yet been attempted. Forming nanoparticles using drug conjugates is a simple operation. It can generally be achieved by coupling the drug to a biocompatible lipid moiety, a process that normally requires a linker if the two components cannot be directly attached. Different types of linkers can be used for coupling drug−lipid moieties, such as labile and nonlabile linkers and, more recently, self-immolative linkers.[26]

Squalene is a good example of a self-assembly inducer. This compound is a terpenoid precursor of cholesterol biosynthesis. Its inertness and biocompatibility, allied to the fact that the two ends can be easily functionalized, make it ideal to obtain squalene derivatives that can subsequently be used to produce drug conjugates capable of self-assembling into nanoparticles.[24] In addition, squalene-based hetero-nanoparticles have proved to be internalized by cancer cells, such as human lung cancer A549 cell lines.[11] A strategy for the synthesis of a DHR-squalene conjugate **2** was, therefore, designed as summarized in Figure 2. The confirmation that compound **2** had been obtained relied on a comparison of NMR results for the synthesis product (^{1}H-, ^{13}C-, and attached-proton-test (APT)) with the NMR spectra of DHR and compound **1**. The NMR spectra of compound **1** (^{1}H NMR and 2D NMR spectra), namely, HSQC and HMBC were in agreement with published literature data[9] and the characteristic NMR shifts previously assigned to DHR.[1] The parent ion detected in the ESI mass spectrum at *m*/*z* 903.72 $[M-1]^+$ confirmed the expected molar mass of compound **2** (904.72 g mol^{-1}).

https://doi.org/10.1021/acsomega.2c05353
ACS Omega 2022, 7, 44180−44186

The nanoparticles obtained through self-assembling of the DHR-squalene conjugate were characterized in terms of diameter, polydispersity index (PI), and ζ-potential (ζ) for 2 months. As shown in Figure 8, the formulation initially showed

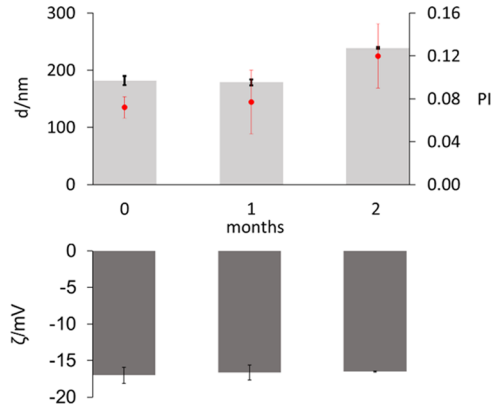

Figure 8. Particle diameter (d, light gray bars), polydispersity index (PI, red dots), and ζ-potential (ζ, dark gray bars) of the DHR-squalene conjugate **2** nanoparticles (n = 3, mean ± SD).

a population with a mean particle diameter $d \sim 182$ nm and $\zeta = -17$ mV. The d values were maintained constant throughout the first month. After 2 months, however, a slight increase in the particle diameter was noted (Figure 8). This increase may reflect a partial aggregation of the self-assemblies.

The PI results also show an increasing tendency over time although the observed change is covered by the uncertainty of the determinations. The values are, nevertheless, small, ranging from 0.072 to 0.12, thus indicating a narrow and homogeneous size distribution (note that although no specific standards have been established, in drug delivery applications, PI < 0.3 is generally considered an acceptable limit for an homogeneous nanoparticle size distribution).[27] The ζ-potential remains essentially unchanged throughout the two-month period. The stability ratio SR = 0.97, obtained from eq 1 after 2 months, is very close to unity, thus indicating that the formulation is rather stable.

SEM analysis revealed that the nanoparticles exhibit a spherical morphology (Figure 9), as had been previously observed for squalene-based hetero-nanoparticles.[28,29] The approximate range of particle diameters obtained from the SEM images agrees with the corresponding DLS results.

Finally, and most noteworthy, the facile dispersion of the DHR-squalene conjugate nanoparticles in phosphate buffer (pH 7.4) gave a strong indication that the insolubility of pure DHR in aqueous media can be overcome through this nanodelivery platform.

CONCLUSIONS

6,7-Dehydroroyleanone (DHR) is an abietane present in the essential oil of *P. madagascariensis*, which has previously been found to exhibit interesting anticancer properties. The present work showed no evidence of DHR polymorphism between ambient temperature and the temperature of fusion (439.6 ± 0.2 K), which is a very important feature in terms of developing a pharmaceutical formulation with highly reproducible properties. It was found, however, that the compound is virtually insoluble in aqueous media, which implies a very poor bioavailability and hinders its use as a drug. Moreover, because

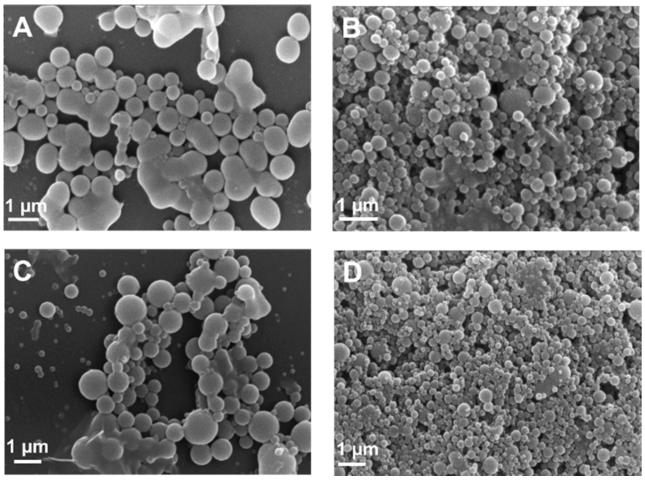

Figure 9. SEM micrographs showing the morphology of the nanoparticles (NPs) formed by self-assembly of the DHR-squalene conjugate **2**. (A, C) NPs (2 mg cm^{-3}); (B, D) NPs (1 mg cm^{-3}).

fusion is accompanied by partial decomposition, strategies to improve the solubility of DHR, such as the production of an amorphous material by, e.g., melting and quench cooling or dispersion in polymeric excipients cannot be used. To overcome this solubility limitation, a conjugate consisting of DHR linked to squalene derivative was synthesized and used to produce self-assembled nanoparticles. The obtained nanosized material showed a narrow and homogeneous particle size distribution and significant stability over time in terms of particle size, polydispersity index, and ζ-potential. Such stability and the facile dispersion in aqueous media (phosphate buffer, pH 7.4) suggest that this nanoparticle material may provide an effective platform to enhance the solubility and bioavailability of DHR to desirable therapeutical levels.

ASSOCIATED CONTENT

Supporting Information

The Supporting Information is available free of charge at https://pubs.acs.org/doi/10.1021/acsomega.2c05353.

CIF file with single-crystal X-ray diffraction structure of 6,7-dehydroroyleanone (DHR) at 167 ± 2 K deposited at the Cambridge Crystallographic Data Center (CCDC) with reference number 2073084 (CIF)

DHR crystal data and structure refinement parameters from the single-crystal X-ray diffraction analysis; details of the TG and DSC analyses and of the DHR and synthesis of the DHR-squalene conjugate (PDF)

AUTHOR INFORMATION

Corresponding Authors

Manuel E. Minas da Piedade − *Centro de Química Estrutural, Institute of Molecular Sciences, Departamento de Química e Bioquímica, Faculdade de Ciências, Universidade de Lisboa, 1749-016 Lisboa, Portugal;* orcid.org/0000-0001-7550-6952; Email: mepiedade@fc.ul.pt

Patrícia Rijo − *CBIOS—Universidade Lusófona's Research Center for Biosciences & Health Technologies, 1749-024 Lisboa, Portugal; Instituto de Investigação do Medicamento (iMed.ULisboa), Faculdade de Farmácia, Universidade de Lisboa, 1649-003 Lisboa, Portugal;* orcid.org/0000-0001-7992-8343; Email: p1609@ulusofona.pt

https://doi.org/10.1021/acsomega.2c05353
ACS Omega 2022, 7, 44180−44186

Authors

Catarina García − *CBIOS—Universidade Lusófona's Research Center for Biosciences & Health Technologies, 1749-024 Lisboa, Portugal; Departamento de Ciencias Biomédicas (Área de Farmacología; Nuevos Ágentes Antitumorales, Acción Tóxica Sobre Células Leucémicas, Facultad de Farmacia, Universidad de Alcalá de Henares, 28805 Alcalá de Henares, Madrid, España*

Carlos E. S. Bernardes − *Centro de Química Estrutural, Institute of Molecular Sciences, Departamento de Química e Bioquímica, Faculdade de Ciências, Universidade de Lisboa, 1749-016 Lisboa, Portugal;* orcid.org/0000-0003-1490-9728

M. Fátima M. Piedade − *Centro de Química Estrutural, Institute of Molecular Sciences, Departamento de Química e Bioquímica, Faculdade de Ciências, Universidade de Lisboa, 1749-016 Lisboa, Portugal; Centro de Química Estrutural, Institute of Molecular Sciences, Instituto Superior Técnico, Universidade de Lisboa, 1049-001 Lisboa, Portugal*

Gaia Fumagalli − *Dipartimento di Chimica, Università Degli Studi di Milano, 20133 Milano, Italy*

Eleonora Colombo − *Dipartimento di Chimica, Università Degli Studi di Milano, 20133 Milano, Italy*

Ana M. Díaz-Lanza − *Departamento de Ciencias Biomédicas (Área de Farmacología; Nuevos Ágentes Antitumorales, Acción Tóxica Sobre Células Leucémicas, Facultad de Farmacia, Universidad de Alcalá de Henares, 28805 Alcalá de Henares, Madrid, España*

Catarina P. Reis − *Instituto de Investigação do Medicamento (iMed.ULisboa), Faculdade de Farmácia, Universidade de Lisboa, 1649-003 Lisboa, Portugal; Instituto de Biofísica e Engenharia Biomédica, Faculdade de Ciências, Universidade de Lisboa, 1749-016 Lisboa, Portugal*

Isabel Correia − *Centro de Química Estrutural, Institute of Molecular Sciences, Instituto Superior Técnico, Universidade de Lisboa, 1049-001 Lisboa, Portugal;* orcid.org/0000-0001-7096-4284

Lia Ascensão − *Centro de Estudos do Ambiente e do Mar (CESAM), Faculdade de Ciências, Universidade de Lisboa, 1749-016 Lisbon, Portugal*

Daniele Passarella − *Dipartimento di Chimica, Università Degli Studi di Milano, 20133 Milano, Italy*

Complete contact information is available at: https://pubs.acs.org/10.1021/acsomega.2c05353

Author Contributions

The manuscript was written with the contributions of all authors. All authors have approved the final version of the manuscript.

Notes

The authors declare no competing financial interest.

■ ACKNOWLEDGMENTS

The authors would like to thank Fundação para a Ciência e Tecnologia (FCT), Portugal, for financial support of this work under the references UIDB/04567/2020, UIDP/04567/2020, UIDB/04138/2020, UIDP/04138/2020, UIDB/00100/2020, UIDP/00100/2020, and PTDC/QUI-OUT/28401/2017 (LISBOA-01-0145-FEDER-028401). The grants UID/DTP/04567/2016, PADDIC 2016, and PADDIC 2017 from ALIES-COFAC, as part of the PhD program in Health Sciences from Universidad de Alcalá and Universidade Lusófona de Humanidades e Tecnologias, have also contributed for this work. I.C. thanks the FCT Investigador program and C.E.S.B. thanks FCT for grant 2021.03239.CEECIND.

■ REFERENCES

(1) Garcia, C.; Silva, C. O.; Monteiro, C. M.; Nicolai, M.; Viana, A.; Andrade, J. M.; Barasoain, I.; Stankovic, T.; Quintana, J.; Hernández, I.; González, I.; Estévez, F.; Díaz-Lanza, A. M.; Reis, C. P.; Afonso, C. A. M.; Pesic, M.; Rijo, P. Anticancer Properties of the Abietane Diterpene 6,7-Dehydroroyleanone Obtained by Optimized Extraction. *Future Med. Chem.* **2018**, *10*, 1177−1189.

(2) Bernstein, J.*Polymorphism in Molecular Crystals*, 2nd ed.; Oxford University Press: Oxford, 2020.

(3) Brittain, H. G.*Polymorphism in Pharmaceutical Solids*, 2nd Ed.; Informa Healthcare: New York, 2009.

(4) Brittain, H. G.*Polymorphism in Pharmaceutical Solids; Drugs and the Pharmaceutical Sciences*; Taylor & Francis, 1999.

(5) Hilfiker, R.*Polymorphism in the Pharmaceutical Industry*; Wiley-VCH: Weinheim, 2006.

(6) Koltzenburg, S.Formulation of Problem Drugs. In *Solubility Enhancment with BASF Pharma Polymers*; Reintjes, T., Ed.; BASF SE: Lampertheim, 2011.

(7) Mengzhu, Z.; Xiaohan, Q.; Zhipeng, Z.; Qian, D.; Qian, L.; Yue, J.; Yuxia, L. A Self-amplifying Nanodrug to Manipulate the Janus-faced Nature of Ferroptosis for Tumor Therapy. *Nanoscale Horiz.* **2022**, *7*, 198−210.

(8) Zhang, J.; Ningning, W.; Qian, L.; Yaxin, Z.; Yuxia, L. A Two-pronged Photodynamic Nanodrug to Prevent Metastasis of Basal-like Breast Cancer. *Chem. Commun.* **2021**, *57*, 2305−2308.

(9) Borrelli, S.; Christodoulou, M. S.; Ficarra, I.; Silvani, A.; Cappelletti, G.; Cartelli, D.; Damia, G.; Ricci, F.; Zucchetti, M.; Dosio, F.; Passarella, D. New Class of Squalene-based Releasable Nanoassemblies of Paclitaxel, Podophyllotoxin, Camptothecin and Epothilone A. *Eur. J. Med. Chem.* **2014**, *85*, 179−190.

(10) Adhikari, P.; Pal, P.; Das, A. K.; Ray, S.; Bhattacharjee, A.; Mazumder, B. Nano Lipid-Drug Conjugate: An Integrated Review. *Int. J. Pharm.* **2017**, *529*, 629−641.

(11) Borrelli, S.; Cartelli, D.; Secundo, F.; Fumagalli, G.; Christodoulou, M. S.; Borroni, A.; Perdicchia, D.; Dosio, F.; Milla, P.; Cappelletti, G.; Passarella, D. Self-Assembled Squalene-Based Fluorescent Heteronanoparticles. *ChemPlusChem* **2015**, *80*, 47−49.

(12) Hensch, M.; Rüedi, P.; Eugster, C. H. Horminon, Taxochinon Und Weitere Royleanone Aus 2 Abesstuischen *Plectruntkus*-Spezies (Labiatae). *Helv. Chim. Acta* **1975**, *58*, 1921−1934.

(13) Bruker Analytical System. Apex 2, 2010.

(14) Sheldrick, G. M. Crystal Structure Refinement with SHELXL. *Acta Crystallogr., Sect. C: Struct. Chem.* **2015**, *71*, 3−8.

(15) Sheldrick, G. M. In *Program for Crystal Structure Solution and Refinement*, SHELXS-97 and SHELXL-97; University of Gottingen: Gottingen, 1997.

(16) Farrugia, L. J. WinGX Suite for Small-Molecule Single-Crystal Crystallography. *J. Appl. Crystallogr.* **1999**, *32*, 837−838.

(17) Macrae, C. F.; Bruno, I. J.; Chisholm, J. A.; Edgington, P. R.; McCabe, P.; Pidcock, E.; Rodriguez-Monge, L.; Taylor, R.; van de Streek, J.; Wood, P. A. Mercury CSD 2.0 − New Features for the Visualization and Investigation of Crystal Structures. *J. Appl. Crystallogr.* **2008**, *41*, 466−470.

(18) Spek, A. L. Structure Validation in Chemical Crystallography. *Acta Crystallogr., Sect. D: Biol. Crystallogr.* **2009**, *65*, 148−155.

(19) Bernardes, C. E. S.; Garcia, C.; Pereira, F.; Mota, J.; Pereira, P.; Cebola, M. J.; Reis, C. P.; Correia, I.; Piedade, M. F. M.; Minas da Piedade, M. E.; Rijo, P. Extraction Optimization and Structural and Thermal Characterization of the Antimicrobial Abietane 7α-Acetoxy-6β-Hydroxyroyleanone. *Mol. Pharm.* **2018**, *15*, 1412−1419.

(20) Abdissa, N.; Frese, M.; Sewald, N. Antimicrobial Abietane-Type Diterpenoids from Plectranthus Punctatus. *Molecules* **2017**, *22*, 1919.

(21) Naman, C. B.; Gromovsky, A. D.; Vela, C. M.; Fletcher, J. N.; Gupta, G.; Varikuti, S.; Zhu, X.; Zywot, E. M.; Chai, H.; Werbovetz, K. A.; Satoskar, A. R.; Kinghorn, A. D. Antileishmanial and Cytotoxic Activity of Some Highly Oxidized Abietane Diterpenoids from the Bald Cypress, *Taxodium distichum*. *J. Nat. Prod.* **2016**, *79*, 598−606.
(22) Razak, I. A.; Salae, A. W.; Chantrapromma, S.; Karalai, C.; Fun, H.-K. Redetermination and Absolute Configuration of 7α-Hydroxyroyleanone. *Acta Crystallogr., Sect. E: Struct. Rep. Online* **2010**, *66*, o1566−o1567.
(23) Cremer, D.; Pople, J. A. General Definition of Ring Puckering Coordinates. *J. Am. Chem. Soc.* **1975**, *97*, 1354−1358.
(24) Fumagalli, G.; Marucci, C.; Christodoulou, M. S.; Stella, B.; Dosio, F.; Passarella, D. Self-Assembly Drug Conjugates for Anticancer Treatment. *Drug Discovery Today* **2016**, *21*, 1321−1329.
(25) Silva, C. O.; Molpeceres, J.; Batanero, B.; Fernandes, A. S.; Saraiva, N.; Costa, J. G.; Rijo, P.; Figueiredo, I. V.; Faísca, P.; Reis, C. P. Functionalized Diterpene Parvifloron D-Loaded Hybrid Nanoparticles for Targeted Delivery in Melanoma Therapy. *Ther. Delivery* **2016**, *7*, 521−544.
(26) Fumagalli, G.; Polito, L.; Colombo, E.; Foschi, F.; Christodoulou, M. S.; Galeotti, F.; Perdicchia, D.; Bassanini, I.; Riva, S.; Seneci, P.; García-Argáez, A.; Via, L. D.; Passarella, D. Self-Assembling Releasable Thiocolchicine−Diphenylbutenylaniline Conjugates. *ACS Med. Chem. Lett.* **2019**, *10*, 611−614.
(27) Danaei, M.; Dehghankhold, M.; Ataei, S.; Davarani, F. H.; Javanmard, R.; Dokhani, A.; Khorasani, S.; Mozafari, M. R. Impact of Particle Size and Polydispersity Index on the Clinical Applications of Lipidic Nanocarrier Systems. *Pharmaceutics* **2018**, *10*, 57.
(28) Fumagalli, G.; Christodoulou, M. S.; Riva, B.; Revuelta, I.; Marucci, C.; Collico, V.; Prosperi, D.; Riva, S.; Perdicchia, D.; Bassanini, I.; García-Argáez, A.; Via, L. D.; Passarella, D. Self-Assembled 4-(1,2-Diphenylbut-1-en-1-yl) Aniline Based Nanoparticles: Podophyllotoxin and Aloin as Building Blocks. *Org. Biomol. Chem.* **2017**, *15*, 1106−1109.
(29) Fumagalli, G.; Giorgi, G.; Vágvölgyi, M.; Colombo, E.; Christodoulou, M. S.; Collico, V.; Prosperi, D.; Dosio, F.; Hunyadi, A.; Montopoli, M.; Hyeraci, M.; Silvani, A.; Lesma, G.; Via, L. D.; Passarella, D. Heteronanoparticles by Self-Assembly of Ecdysteroid and Doxorubicin Conjugates to Overcome Cancer Resistance. *ACS Med. Chem. Lett.* **2018**, *9*, 468−471.

https://doi.org/10.1021/acsomega.2c05353
ACS Omega 2022, 7, 44180−44186